의학물리. 제6권 2호 1995

Analysis of dose from surface to near the buildup region in the therapeutic X-ray beam

Young Woo Vahc, Ph. D.
Yonsei University Wonju College of Medicine Department of Physics

Abstract

The absorbed dose and contaminant electron distribution of therapeutic X-ray beam (15MV photon) was studied with a half blocked beams of 30×30cm^{2}and field size ranging from 5×5 to 30×30cm^2. For a 15MV photon beam energy, the value of the depth of dose maximum, d_{max}, gradually decrease with increasing field size from 5×5 to 30×30cm^2 due to mainly by contaminant electrons which are produced in the flattening filter and scattered by collimator jaws, tray holder〔Lucite〕, blocking block and air. The results suggest that separate dosimetry data should be kept for blocked and unblocked field. The inherence of the contaminant electrons to the open field depth of maximum dose can lead to mistaken results if attenuation measurements are made at that depth. A nurmerous contaminant electrons mainly were distributed as shape of corn in the central photon beam and their path length in the water were shorter than 30mm because of the electrons energy having around 6MeV. These results clearly appears that the substraction of scattered electrons (electrons and positrons) from the total depth dose curve not only lowers the absolute dose in the bulidup region and surface dose, it also causes a shift of d_{max} to a deeper depth. In the terapeutic high energy photon beam, the absorbed dose near the buildup region is the combined result of incident contaminant electrons and phantom generated electrons.

1. INTRODUCTION

The contaminant electrons must be produced in a therapeutic linear accelerator (linacs)when primary photons interact with machine components such as the flattening filter, beam monitor, collimator jaws, etc. The radiation contaminants with various low energies include scattered photons, electrons and positrons due to mainly pair production process. The depth of dose maximum, d_{max}, of therapeutic photon beams produced by linacs is a function of both beam energy and field size. For a given field size, d_{max} increases with photon beam energy and a given beam energy, many of these works have reported a si gnificant increase in surface dose and a corresponding shift of the d_{max} toward the surface when the field size is increased at normal treatment source-surface distances(SSDs). The energy dependence of d_{max} is of major clinical importance since it determines the extent of the dose buildup region, The skin-sparing effect has long been recognized as one of the most beneficial characteristics of therapeutic radiation beams. This clinical advantage may be compromised in some cases by the presence of low energies contaminant electrons in the central beam due to scattered radiation from mainly the gantry head. Several experiments have yielded convincing evidence that the beam contamination which gives rise to this increased skin dose consists primarily of forward-scattered electron.

These results clearly show that the contaminant electrons are the primary cause for the d_{max} shift and the dose increase in the buildup region with increasing field size.

The contaminant electrons have an effect on the buildup region of therapeutic photon beams and, when subtracted from the total depth dose curve, will give the dose distribution of the pure photon beam affected only by phantom scatter. The substraction of contaminant electrons from total depth dose curve not only lowers the absolute dose in the buildup region, it also causes a shift of d_{max} to a deeper depth. The dose from phantom generated electrons increase exponentially with depth from surface to buildup region, but the dose from contaminant electrons decreased rapidly with depth with an attenuation coefficient within 30mm depth length.

2. MATERIALS AND METHODS

All experiments were done with a 15-MV photon beam from a dual energy linear ac celerator (Clinac 1800, Varian). Field sizes were defined by the rectangular collimators of the linacs and ranged from 5×5 to $30 \times 30 cm^2$, covering the complete range of radiation fields used in all types of radiotherapy. The distribution of scattered dose (contaminant electrons, positrons and scattered lower energy photon) was measured by loading 10cm shielding alloy blocks in the photon beam at the level of tray holder on the Lucite plate of the 15MV linac to produce half-blocked and full-blocked fields.

The thimble chamber (PTW-0.3cm^3, Model No. M233641) was used in Multi-Data 3D water phantom for percent depth dose measurements from surface to 20.0 cm and beam profile as function of depth variation from surface to 3.0cm below. The electrometer(Victoreen 500) was used to measure the charge collected on the measuring electrode of the ionization chamber. The central and off-central axis depth dose data for with half-blocked beam were obtained by scanning the beam in steps of 1.0mm each 1cm interval from center to off-center. An average of 70 points for steps, at each interval, was obtained for analysis. There is a half-shielding block (10cm thick shielding alloy) in the water phantom to avoid the scattered photons and contaminant electrons going to the ionization chamber for 15MV photon beam at $30 \times 15 cm^2$ half-blocked field size.

To measure the signal of half-blocked beam profile at water phantom is to calculate the distribution of contaminant electrons and scattered photons as function of depth and around 15MV photon central beam. The most of contaminant electron mainly were concentrated in the center as like corn shape distribution.

3. RESULTS AND DISCUSSION

The apparatus shown in Fig. 1 is used for the measurements of the head scatter components, tray holder (Lucite) and air. Fig.1-A appears the open radiation beam of linear accelerator gantry head with tray holder. The schematic diagram traces incident photons from the X-ray source, through the flattening filter and transmission ionization chamber, past the collimator jaws and to the thimble ionization chamber (PTW-0.3cm^3, M233641)in a water phantom at a 100cm SSD. The charge collected by the ionization chamber on the central axis and off-center for percent depth dose in the water phantom is due to primary photons, contaminant electrons and/or photon machine head scatter and phantom scatter.

In Fig. 1-B, if appears that the setup used to eliminate the charge collected due to primary photons and phantom scatter from the signal read by the ionization chamber. A 10cm thick shielding alloy block large enough to block half of the open beam was placed into the beam at the level of the linac accessories tray holder with Lucite plate. The 10cm shielding alloy block in the water phantom was positioned at 100cm SSD out of the shadow of the half-block such that the upper half-block edge coincided with the edge of the lower half-block. The purpose was to separate the head scatter component on the central or off-center axis for comparision with the total percent depth dose measurement at the same position. To eliminate the contribution of the primary beam, the ionization chamber must lie in the shadow of the upper half-block. The only radiation that could then reach the detector was that transmitted through the upper half-block, scattered in the collimator jaws, or scattered in the volume of air of Lucite plate irradiated by one half of the primary beam. The role of lower half-block is to prevent from the buildup effects in the water phantom coming from the primary photons, scattered photons and contaminant electrons in the open beam.

In Fig. 1-C & D, to account for the distribution of contaminant electrons as function of the depth and near the central beam, we measured the beam profile of half-block photon beam without lower half-block in the water phantom.

In Fig. 2 shows the method used for determining the total head scatter and elsewhere for a 30×30cm^2 open 15MV field from the measurements with the experimental setup of Fig. 1-A and 1-B. In Fig.2, all curves represent the radiation scattered from the collimator jaws, tray holder and air but also include the primary radiation which is transmitted through the half-block. All depth dose curves become identical for depth beyond 40.0mm in water phantom indicating that the scattered radiation component is fully absorbed by the superficial layers of the water phantom. The most of scattered radiation are concentrated in the central beam and rapidly decay within 30.0mm means that these curves represent contaminant electron depth dose and a long flatten tails of depth dose curve represent

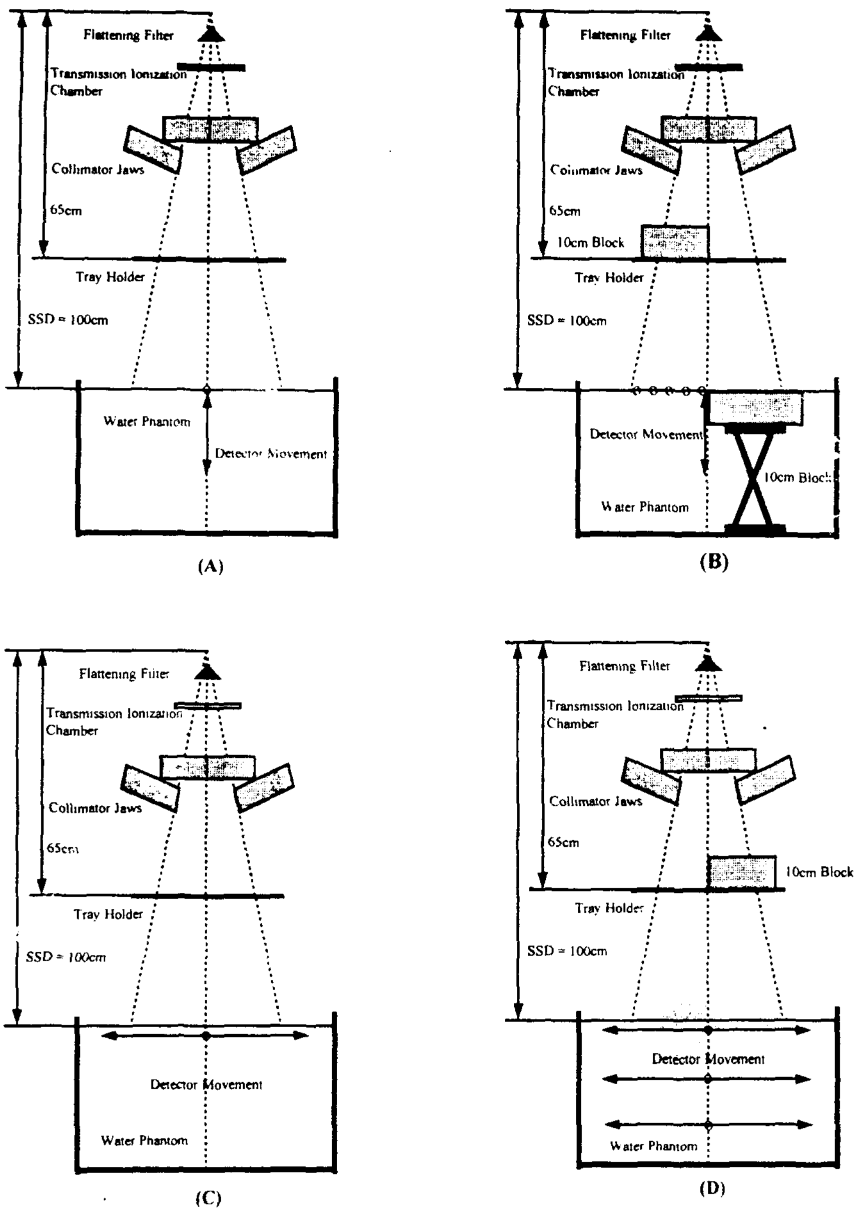

Fig.1. The schematic diagram of the experimental setup for measuring the dose distribution in the buildup region. Part(A)shows the setup for measuring the dose of full open beam in the water phantom with tray holder(Lucite), Part(B)shows the setup used to measure the scatter dose from the gantry head with the upper half-block on the tray holder and 10cm shielding alloy block in the water to prevent from the primary photon and scattered lower energy photon's buildup effect, Part(C) 1&(and) (D)show the setup to measure the beam profiles for the distribution of scattered radiation components.

lower energy scattered photon beams.

From the particular shape of curve B in Fig. 2 we can deduce that the scattered radiation is of relatively low energy, however, if could represent low energy photons or contaminant electrons. With a simple experiment, described and performed previously[2],where the attenuation of a radiation beam is measured in lead and in poltstyrene, we confirmed previous findings that the meaured scattered radiation component consists of electrons rather than photons. Fig. 2 also appears the lack of buildup in the scatter curves. This indicates the predominance of electrons in the scattered radiation, showing that photons do not substantially contribute to the contamination scatter component. In Fig. 3, we plot five depth dose distributions for a 15MV photon beam and a fields of $30\times30cm^2$ open and $30\times15cm^2$ half-block beam at 100 SSD. Curve A represents the dose distribution measured with the open beam setup of Fig. 1-A, and curve B represents the dose distribution measured with the half-block beam out of shadow side setup of Fig.1-B without lower half-block shielding alloy. Curve D included scattered photons is the percent depth dose at the shadow position (off-center 10.0mm)of the upper half-block, curve E represents the contaminant electron depth dose subtracted from scattered lower energy photon to curve D, curve C results from a substraction of the contamination curve E from the measured total depth dose curve B.

The subtraction of curve E from curve B not only lowers the absolute dose in the buildup region, if also causes a shift of d_{max} to a deeper depth as indicated in Fig.3. The electron scattered contamination discussed above has an effect on the buildup region of megavoltage photon beams and, when subtracted from the total depth dose curve by simulation, will give the dose distribution of the clean photon beam affected only by phantom scatter. It is interesting to note that the surface dose drops from an initial high to final low as we remove contaminant electrons by simulation.

In Fig.4 all measured percent depth doses were plotted as variation of side of square field for 15 MV photon beam in the field size range from 5×5 to $30\times30cm^2$. The d_{max} dependence on beam energy and field size due to contaminant electrons is shown. For a constant small or large field size, d_{max} increases with increasing beam energy clearly. For a given energy, with increasing field size, the values of d_{max} decrease slowly. For measured percent depth dose curves, the values of d_{max} are 29.0 and 16.0mm for the field size 5×5, $30\times30cm^2$, respectively. The magnitude of the d_{max} shifted as many as 13.0mm toward the surface. At large field sizes, contaminant electrons from the gantry, tray holder (Lucite)and air may contribute a substantial amount to the dose in the buildup region within 30.0 mm depth. The contaminant electrons which soften the therapeutic photon beam at large field sizes could be measured and then subtracted from the total measured dose.

Clearly, megavoltage radiation beams used in radiation therapy contain a contaminant electrons which is negligible for small radiation fields but slowly increases with field size to reach a size able proportion of the total dose in the buildup region for large fields.

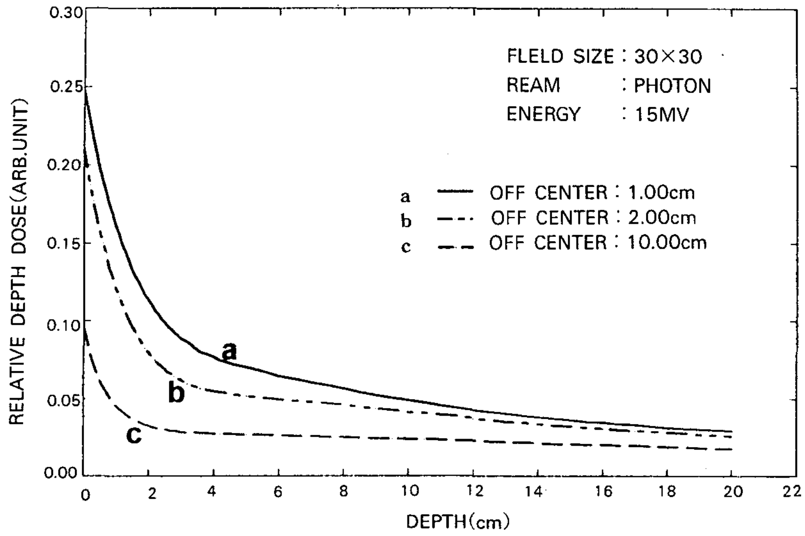

Fig.2. Technique used to obtain the percent depth doses due to contaminat electrons and scattered low energy photons for a 15MV, 30×15cm2half-block beams. Curve(a), (b) and (C) are the percent depth doses at 1.0, 2.0, 10.0cm, respectively toward the off-center under the shadow of upper half-block with the setup Fig.1-B.

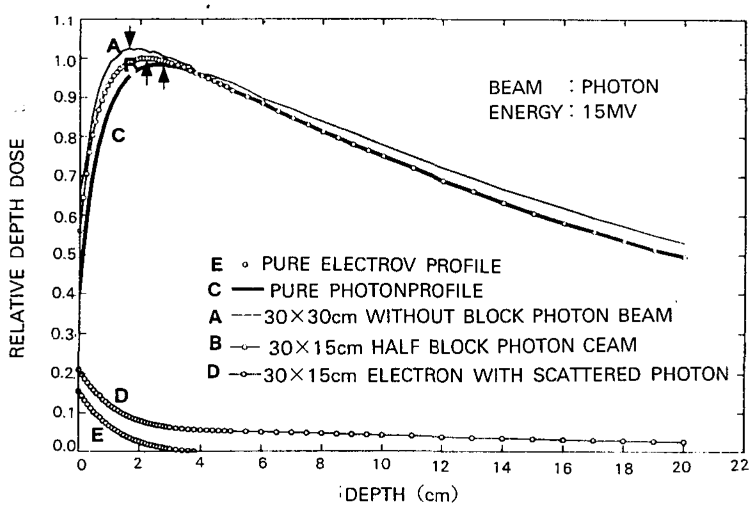

Fig.3. Data for for the buildup region fo a 30×30cm2open 15MV photon beam plotted as the percent depth doses versus the depth in a water phantom. Curve (b) represent s the total depth dose distribution measured with the setup Fig.1-A. curve(e) represents the electron scatter component, and curve (c) represents the depth dose data accounting for phantom scatter but with contaminant scatter removed. The data arrows on the curve (a), (b) and (c) represent the position of d_{max} for th three curves. The d_{max} has a more larger depth with removed contaminant scatter.

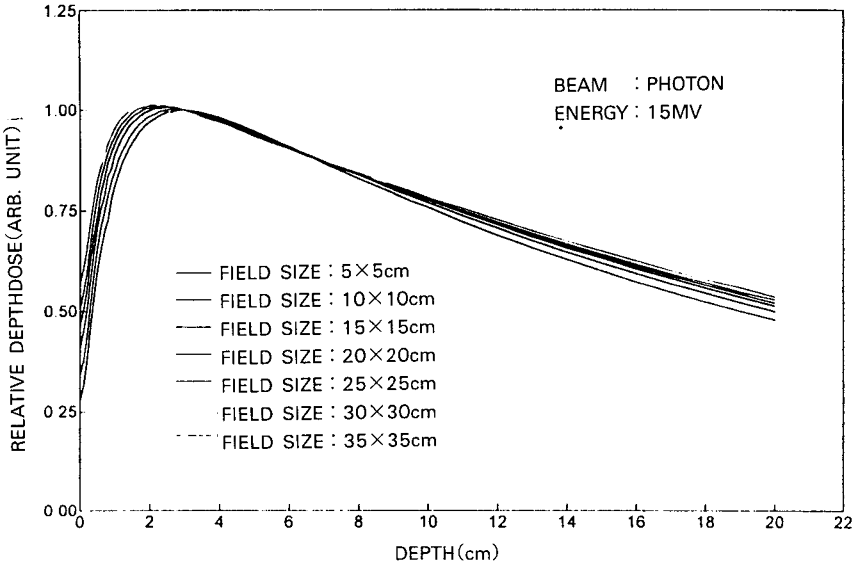

Fig.4. Depth of dose maximum as a function of field sizes for a 15MV PHOTON BEAM. The shift in each d_{max} to shallower depths, as field size is increased, is due to the increase in contaminant electrons.

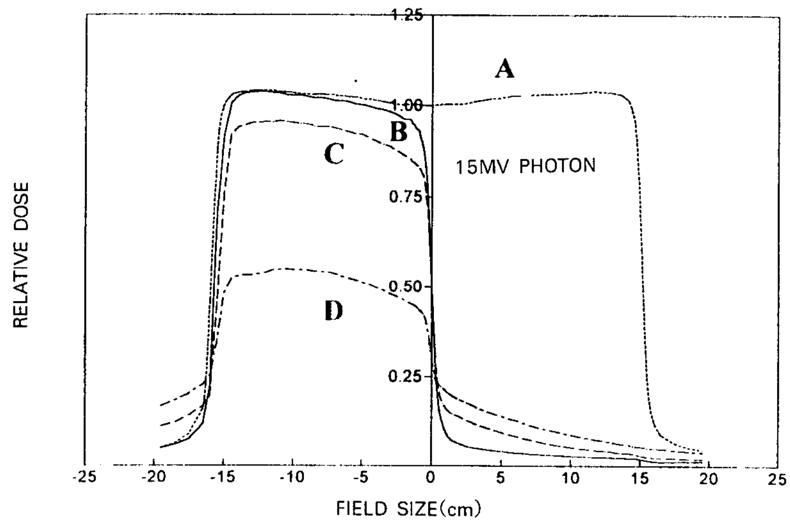

Fig.5. The dose distribution of fhalf-block beam profiles without 10cm shielding alloy block in the water phantom with setup Fig.1-D. Curve A is the normal full beam profile, curve B,C and D represent the dose distribution of half-block beam profile at depth surface, 1.0cm, 3.0cm, respectively.

The contaminant electron is the most pronounced on the surface and becomes negligible at depths around the nominal d_{max} of the X-ray beam, which is on the order of the range of the most energetic electrons produced by photon in the phantom material.

In Fig.5, we plot four beam profiles. The curve A represents a normal dose distribution of beam profile measured with the full open beam setup Fig.1-C and curve B, C and D represent the dose distribution of half-block beam profile to measure the distribution of contaminant electrons and scattered lower energy photons with setup of Fig.1-D at depth surface, 1.0cm, 3.0cm respectively. Curve D appears that contaminant electrons and scattered lower energy photon at the surface level are spread widely, but they are mainly concentrated in the central beam. For curve B, a lot of contaminant electrons are decreased rapidly within 3.0cm path length by fully attenuation, but a small amounts of scattered lower energy photon still presents and represents as like long flat tail. We confirmed previous findings that the measured scattered radiation component consists of electrons rather than scattered low energy photons.

4. CONCLUSIONS

The high energy and pure photon beams not only spare the superficial tissues but also enhance the delivered at depths, but, due to contaminant electrons, the beam may degrade to some degree for large field sizes. The subtraction of contaminant electrons from the normal therapeutic radiation beam not only lowers the absolute dose in the buildup region and especially entrance dose, it also causes a shift of d_{max} to a larger depth and will give the dose distribution of the clear photon beam affected only by phantom scatter. This study is for preparatory experiment to remove the contaminant electrons and positrons in the therapeutic radiation beam.

Acknowledgments

I deeply thank Chul W. Joh, Yong H. Lee and Jong J. Choi. I also would like to express my thanks to the Department of Radiation Oncology at Yonsei University Wonju College of Medicine.

5. REFERENCE

1. G Arcovito, A. Piermattei, G. D′ Abramo, and R. Andreasi Bassi, Dose measurements and calculations of small radiation fields for 9-MV X rays, Phys. Med. 12, 779−784(1985)
2. P. J. Biggs and C. C. Ling, Electrons as the causes of the observed d_{max} shift with field size in high energy photon beams, Med. Phys. 6, 291 (1979)
3. D. J. Dawson, Phys. Med. Biol. 21, 226 (1976)
4. H. E. Johns, etal, Br. J. Radiol. 25, 302 (1952)
5. K. E. Sixel and E. B. Podgorsak, Buildup region and depth of dose maximum of megavoltage X-ray beams, Med. Phys. 21 (3), 411−416 (1994)

6. D. M. Galbraith and J. A. Rawlinson, "Direct measurement of electron contamination in cobalt beams using a charge detector." Med. Phys. 12, 273−280 (1985)

표피로 부터 buildup 영역까지 흡수되는 암치료용 방사선의 선량분석

박영우

연세대학교 원주의과대학 물리학교실

암치료용 방사선(15 MV의 에너지를 갖는 광자선)속에 있는 흡수선량과 불순전자 또는 산란 광자에 관한 분포를 광자선 면적 크기에 따른 변화와 광자선 면적을 반만 차폐시킨 선속에 대하여 연구 조사하였다. 광자선의 에너지를 15MV로 주어질때 광자선 최대 흡수깊이 d_{max} 값은 광자선의 면적을 증가시키면 시킬 수 록(5×5에서 30×30cm^2)d_{max} 값은 감소된다. 이는 광자선 즉 방사선을 발생시키는 가속기 기계 속에 있는 여러 부품 (flattening filter, collimator jaws, tray holder,······)과 상호작용하여 형성 된 불순전자로 인하여 d_{max}값이 표피쪽으로 이동되어 buildup 영역에 높은 선량흡수를 갖게 된다. 최대 흡수깊이 값을 계산할 때 이러한 현상을 고려하지 않으면 그릇된 data 값을 갖는다. 대부분의 불순 전자는 광자선 중심에 주로 분포하며 그 진행거리는 30.0mm이하의 짧은 거리를 갖는다. 이 불순전자가 30.0mm 이내(즉 buidup 영역)에 전부 흡수되므로 buidup 영역은 높은 선량흡수를 갖게되어 해를 주게된다. 그러므로 이러한 불순전자를 제거 시키므로서 buidup 영역에 낮은 선량 흡수를 갖을 뿐 아니라 d_{max} 값도 역시 깊은 곳까지 이동시켜 치료에 효과적인 방법이 창출된다.